ICAST2014 #054

Adaptive Damage Localization and Accuracy Evaluation for a Composite Aircraft Panel

Shengbo Shan[1], Jinhao Qiu[1*], Chao Zhang[1],Hongli Ji[1]

[1] The State Key Lab of Mechanics and Control of Mechanical Structures, Nanjing University of Aeronautics and Astronautics, Nanjing, 210016, China

Abstract

Structural health monitoring with active Lamb waves is a promising technology due to its potential of covering large monitoring areas with few sensors. However, for complex composite structures, the high signal complexity inherent to the wave propagation presents the main challenge on the application of this technology. In addition, it's not easy to determine the exact group velocities of Lamb waves due to the anisotropic property of the composite material and the limited resolution of the monitoring system. To locate damage on this complex structure, this paper presents a damage monitoring method based on the most frequently-used delay-and-sum algorithm. To improve the adaptiveness of the delay-and-sum imaging method for this complex structure, a valid data extraction strategy is introduced to reduce the influence of boundary reflection which deteriorates the monitoring accuracy. Concerning the uncertainty of the measured group velocity of Lamb waves, a localization accuracy evaluation process is carried out to analyze the relationship between the localization error and the preset velocity. Specifically, a composite stiffened panel with a bonded piezoelectric sensor array is researched in this study. Experimental results verify damage can be located accurately by the proposed method.

1. INTRODUCTION

Aircraft panel structures tend to suffer from the stress caused by large changes in humidity, temperature, pressure, speed, and loading conditions. The stress may significantly reduce the service life of traditional metal panels. For substitution, carbon fiber-reinforced polymer (CFRP) is widely researched for aircraft panel manufacturing thanks to its properties like high strength, low density, corrosion resistance and high temperature tolerance.[1,2] However, transition to this relatively new material poses challenges. When it is applied with shear load or out-of-plane tensile load, CFRP laminate is vulnerable to delamination and matrix crack. Usually, these invisible inner damages are hard to be detected and they may lead to the sudden destruction of the whole structure. Therefore, it is becoming increasingly important to develop systems capable of monitoring the invisible defects in the structure.

Structural health monitoring (SHM), as an online and nondestructive technology, appeals to a lot of researchers.[3,4] Among various SHM tools, the Lamb wave-based active monitoring method is regarded as

*Jinhao Qiu, The State Key Lab of Mechanics and Control of Mechanical Structures, Nanjing University of Aeronautics and Astronautics, Nanjing, 210016, China. Email: qiu@nuaa.edu.cn

one of the most promising SHM methods due to its advantages like high sensitivity to damage and large monitoring range. Since the method was proposed, it has been practiced to detect various kinds of damage in composite structures, such as holes and notches, delamination, crack and so on.[5-8]

To obtain the damage information from the original wave signals, various splendid monitoring algorithms are designed, including damage index (DI),[9,10] time reversal,[11] statistical modeling[12] and damage imaging algorithm.[13] In particular, one of damage imaging algorithms named the delay-and-sum algorithm is widely researched[14-18]. This method uses an interpretable and intuitive image to reflect the damage location in the structure. It is firstly proposed by Wang et al.[14] to locate the bonded mass on an aluminum plate. C T Ng and M Veidt[17] measure the group velocities in different directions of a composite plate and apply the delay-and-sum algorithm to detect the defect in the plate. Based on the delay-and-sum algorithm, Wang et al.[18] propose a time-reversal imaging algorithm for a composite plate to enhance the signal-to-noise ratio and improve the imaging resolution by weakening the influence of dispersion of Lamb waves.

However, when it comes to composite aircraft panels, there are a few issues limiting the direct use of the delay-and-sum imaging algorithm. The propagating characteristics of Lamb waves in the aircraft panel are complex due to the existence of the stiffeners.[19] In addition, the high damping property of CFRP result in the rapid attenuation of Lamb waves which deteriorates the monitoring accuracy. Furthermore, it is almost impossible to determine the exact group velocity of scattering Lamb waves due to the anisotropic property of the composite material and finite resolution of the monitoring system. It is necessary to quantitively analyze the influence of the uncertainty of the preset velocity on the localization accuracy.

Motivated by the above-addressed challenges in today's SHM for CFRP aircraft panel structures, a damage monitoring method is proposed using piezoelectric sensor-actuators. First, the delay-and-sum imaging algorithm is presented. Second, a valid data extraction strategy is designed with the aim of reducing the influence of boundary reflections. As a part of the damage imaging method, the strategy is designed to make the damage imaging method adaptive to the monitoring structure. The integrated damage imaging method is then applied to locate the damage in the monitoring area. At last, a further evaluation is conducted to find out the influence of preset velocity on localization accuracy.

2. METHODOLOGY

2.1 Delay-and-sum imaging algorithm

The delay-and-sum imaging algorithm uses residual signals (measured signals subtracted by baseline signals) which are delayed and summed to obtain the damage possibility of each spatial point in the structure. Damage image is then plotted according to the value of the damage possibility. The algorithm can be divided into three steps.

The first step is to calculate the expected arrival time of every point for all actuator-sensor paths. For a point in the structure, the arrival time of a signal traveling from actuator i at (x_i,y_i) to the point at (x,y) and on to sensor j at (x_j,y_j) can be calculated as

$$t_{ij}(x,y) = t_{\text{off}} + \frac{\sqrt{(x-x_i)^2+(y-y_i)^2}+\sqrt{(x-x_j)^2+(y-y_j)^2}}{v_{\text{s}}} \tag{1}$$

where t_{off} is the time offset caused by the exciting process and it is approximately equal to half of the length of the exciting signal and v_{s} is the preset velocity of the monitoring system. Normally, this value is

considered as the actual group velocity of Lamb waves in the structure v_a. However, in this study, the two terms are diacritical strictly.

The next step is to obtain the wavelet coefficient modulus of the residual signals. As different actuator-sensor paths have different sensitivity to damage, residual signals must be normalized first. It ensures that all actuator-sensor paths provide sufficient damage information in the damage imaging process. The normalization process can be expressed as

$$\overline{R(t)} = \frac{D(t) - H(t)}{\max(\text{abs}(D(t) - H(t)))} \tag{2}$$

where $D(t)$ and $H(t)$ are the measured response signal and baseline signal respectively. Complex Morlet wavelet transform is applied to the normalized residual signals to extract the modulus of the wavelet coefficient for further imaging process.[20] The coefficient of the wavelet transform $CWT(a,b)$ is expressed as

$$CWT\left(a,b \mid \overline{R(t)}\right) = \frac{1}{\sqrt{a}} \int_{-\infty}^{+\infty} \overline{R(t)}\ \psi^*\left(\frac{t-b}{a}\right) \mathrm{d}t \tag{3}$$

$$\psi(t) = \frac{1}{\sqrt{\pi\gamma}} e^{j\omega_0 t} e^{-t^2/\gamma} \tag{4}$$

where a and b are the scale and translation factors. a is calculated by $\omega_0 / 2\pi f_a$ and f_a is the frequency to be analyzed. $\psi^*(t)$ represents the conjunction of $\psi(t)$ which is the complex Morlet wavelet mother function. ω_0 donates the angular central frequency and γ is the width of Gaussian window. In this study, only the modulus of wavelet coefficient with a fixed scale factor c is concerned and it is denoted as

$$E(b) = \text{abs}(CWT(c,b \mid \overline{R(t)})) \tag{5}$$

The final step is to calculate the damage possibility of every point and obtain the damage image of the monitoring area. Each residual signal is delayed by the calculated time $t_{ij}(x,y)$. Signals form all actuator-sensor paths are summed to obtain the damage possibility of each spatial point. In the damage image, the possibility is set to be the pixel value, as

$$P(x,y) = \sum_{i=1}^{N-1} \sum_{j=i+1}^{N} E(t_{ij}(x,y)) \tag{6}$$

where N denotes the number of the sensors in the monitoring area.

2.2 Valid data extraction

When Lamb waves run into stiffeners or the boundaries, they will be reflected. This phenomenon poses the main challenge for signal processing that reflected signals may be mistaken for damage information. As a result, the length of response signals for SHM requires careful consideration. A long response signal may unexpectedly contain reflection while a short one will probably lose damage information. To reach a compromise, the concept of monitoring radius of actuator-sensor path is

introduced. It is defined as the length of the long axis of the ellipse within which the actuator-sensor path can provide effective damage information, as is shown in Fig.1(a). In this paper, a two-step valid data extraction strategy is proposed.

The first step is to design the appropriate monitoring radius which is equivalent to deciding the maximum length of the response signals. Fig.1(b) illustrates the designing strategy for monitoring radius. For the actuator-sensor path A-D, the ellipse corresponding to the monitoring radius passes through the midpoint of the short edge of the rectangular monitoring area. This strategy ensures that for each point in the monitoring area, at least three actuator-sensor paths can provide damage information for the point. Meanwhile, the length of response signals is as short as possible and the influence of reflection of Lamb wave is diminished to a fairly large extent. The maximum length of response signals is estimated as:

$$t_{\max} = \frac{r_{\mathrm{mr}}}{v_{\mathrm{s}}} + 2t_{\mathrm{off}} \tag{7}$$

where r_{mr} donates the monitoring radius.

(a) (b)

Figure 1. (a) Sketch of monitoring radius; (b) designing strategy of monitoring radius

After the first step, there may still be reflection parts in the response signals. However, when damage is close to the actuator-sensor path, the scattering wave packet caused by damage can be separated from the residual signal and it is usually the first arrival. In this case, the signals will be truncated again to obtain the optimal length for damage localization. The optimal length of the response signals is expressed as:

$$t_{\mathrm{optimal}} = \begin{cases} t_{\mathrm{fa}} + t_{\mathrm{off}} & (t_{\mathrm{fa}} < \dfrac{r_{\mathrm{mr}}}{v_{\mathrm{s}}} + t_{\mathrm{off}}) \\ t_{\max} & (\text{otherwise}) \end{cases} \tag{8}$$

where t_{fa} donates the time of the first arrival.

2.3 Evaluation of localization accuracy

When locating the damage with the delay-and-sum algorithm, the parameters to be set to the system are the group velocity of Lamb waves and the coordinates of the sensors. In the monitoring system, the

coordinates of the sensors can be precisely measured while it is almost impossible to match the preset velocity with the actual velocity. Obviously, the measurement error of velocity is unavoidable due to the limited resolution of the monitoring system. In the following section, the extent of the localization accuracy deterioration caused by the deviation of the preset velocity is researched. Four steps are designed in the evaluation process.

Step 1: It is assumed that the actual damage locates at a certain point (x,y) in the monitoring area. The normalized residual signals can be ideally reconstructed by shifting the exciting signal according to the geometric characteristics of the monitoring area and the actual group velocity.

Step 2: A deviation p of the actual velocity is considered and the resulting velocity is set to the monitoring system.

$$v_s = v_a(1+p) \tag{9}$$

Step 3: The delay-and-sum algorithm is carried out to obtain the corresponding damage image with the reconstructed residual signals. In the damage image, the calculated damage position is usually regarded as the point where the pixel value reaches the maximum. The distance between the assumed actual damage position (x,y) and the calculated damage position ($x_{\text{calculated}}$,$y_{\text{calculated}}$) is defined as the localization error.

Step 4: The process is conducted to every point in the monitoring area, resulting in the localization error distribution $LED(x,y|p)$ of the monitoring area for a given velocity deviation:

$$LED(x,y|p) = \sqrt{(x-x_{\text{calculated}})^2 + (y-y_{\text{calculated}})^2} \tag{10}$$

3. EXPERIMENTAL SET-UP

3.1 CFRP aircraft panel

The structure of the CFRP aircraft panel is shown in Fig. 2(a). The composite laminates consist of eight layers in a $[0°/90°/+45°/-45°]_s$ stacking sequence. There are several T-shaped stiffeners boned on the panel. Four piezoelectric sensors are attached to the panel covering a monitoring area of 130×220 mm^2. Fig. 2(b) illustrates the labels of the four sensors and the sketch of the monitoring area.

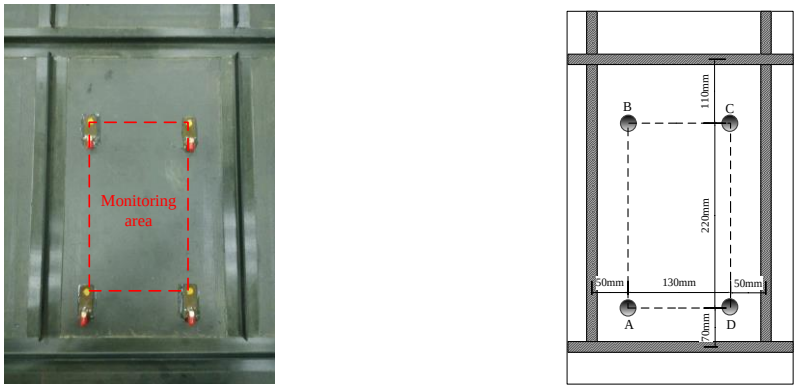

(a) (b)

Figure 2. (a) CFRP aircraft panel; (b) schematic diagram of the monitoring area

3.2 Monitoring system

Fig. 3 illustrates the experimental platform of the damage monitoring system. Firstly, the computer commands the NI-PXI5412 signal generating module to output an exciting signal. Secondly, as the signal is amplified by the power amplifier and applied to the piezoelectric transducer, Lamb waves will be excited in the panel. The channel switch module is designed for making sure that each piezoelectric transducer works as an actuator in a certain order. The monitoring efficiency will be highly improved by this design. Thirdly, response signals pass through the signal conditioner and acquired by the NI-PXI5105 data acquisition module. The signal conditioner is integrated with a voltage amplifier and a band-pass filter. Finally, response signals are stored in the computer and analyzed by the designed algorithm.

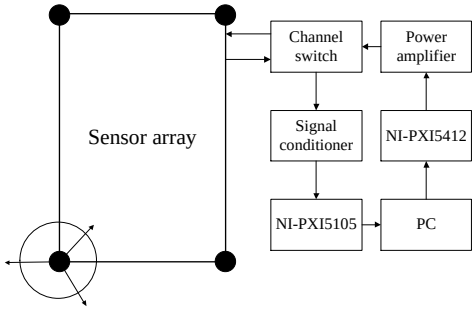

Figure 3. The experimental platform for the damage monitoring system

The exciting signal is a modulated five-cycle sine burst. It is a narrow-band signal which can be expressed as

$$f(t) = A\sin(2\pi f_c t)(1-\cos(\frac{2\pi f_c t}{5})) \tag{11}$$

where A donates the amplitude and f_c represents the central frequency of the signal (60 kHz in this study). At this frequency, A_0 mode amplitude is dominant in the response signals, which is preferred in health monitoring. The exciting signal with the original amplitude of 1 V is amplified by the power amplifier to 60 V. The data acquisition module samples at 1 MHz and 700 points are recorded for every channel. The response signals are amplified (100 times) and band-pass filtered (500 Hz-200 kHz) by the signal conditioner.

3.3 Group velocity measurement

As the composite structure is anisotropic, the group velocities of Lamb wave vary in different directions. When measuring the velocities in this structure, the time of flight (ToF) is required. Hence, the complex Molert transform is applied to the response signals to extract their envelopes.[21] As the complex Morlet wavelet is a narrow-band signal, this process can diminish the influence of noise.

During the velocity measurement, Sensor C performs as the actuator and the response signals of Sensor A, B and D are acquired. These signals are processed with the complex Morlet wavelet transform and the modulus of the wavelet coefficient is shown in Fig. 4. The propagation time of A_0 mode Lamb wave is obtained to calculate the corresponding group velocity. As a result, the velocities in the three different directions are 1123 m/s, 1111 m/s and 1182 m/s respectively in this case. However, for the

monitoring system, an 1 μs error in the ToF may lead to more than 10 m/s error in the calculated velocity. Therefore, it is assumed that there is no significant difference within the three measured velocities in three directions and the monitoring system uses one value for all directions. Finally, the average of the three calculated velocities is regarded as the group velocity of Lamb wave in the CFRP structure, in this case, 1139 m/s. This average processing method will be evaluated in the following localization accuracy evaluation section.

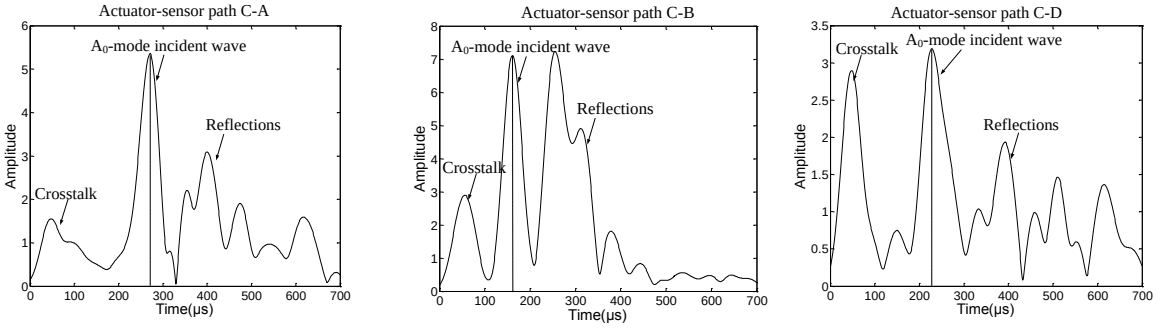

Figure 4. The complex Morlet wavelet coefficient modulus of the response signals received by Sensor (a) A; (b) B; (c) D when Sensor C performs as the actuator

4. RESULTS

In order to validate the monitoring algorithm by detecting the multi-damage in different situations, artificial damages are introduced with a kind of solid adhesive tape as thick as 2mm. It has the same effect as actual damage to interrupt the geometry continuum of the monitoring structure.

4.1 Valid data extraction and damage localization

Specifically, a typical residual signal and the modulus of its wavelet coefficient are shown in Fig. 5(a) and Fig. 5(b). The amplitude of reflection part is as large as that of the scattering wave packet caused by damage. Fig. 5(c) and Fig. 5(d) illustrate the signals after valid data extraction according to equation (8). It can be predicted the localization accuracy will be significantly improved by this strategy.

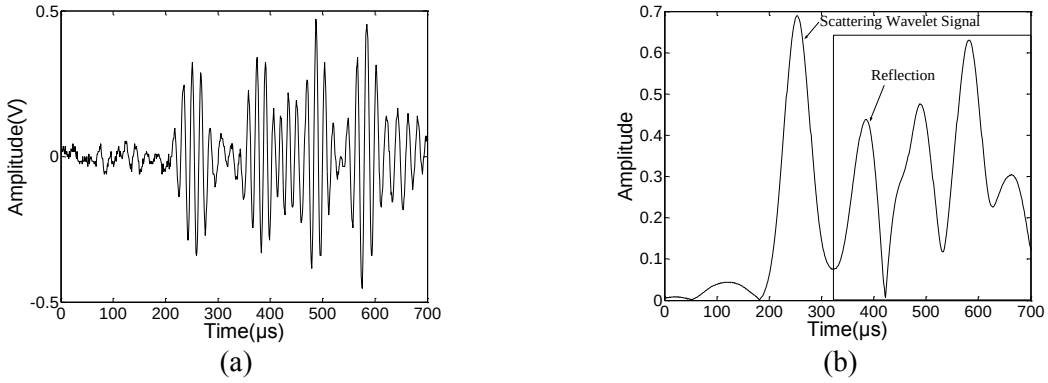

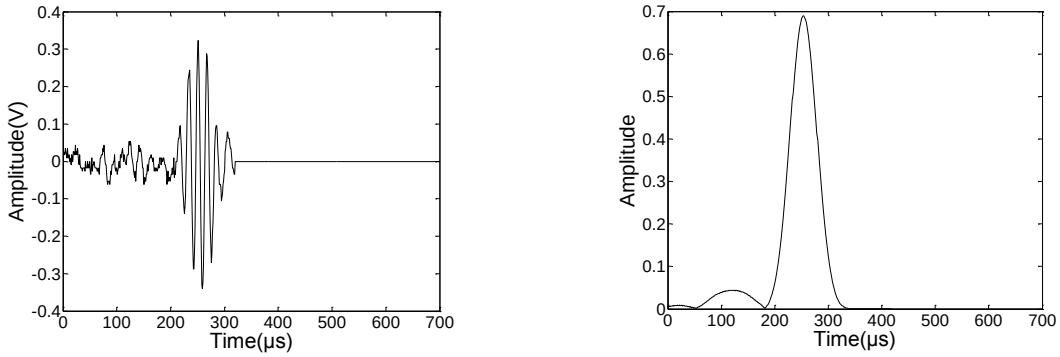

(c) (d)

Figure 5. (a) A typical residual signal containing reflections; (b) the complex Molert wavelet coefficient modulus of the residual signal; (c) residual signal after valid data extraction; (d) the complex Molert wavelet coefficient modulus of the residual signal after valid data extraction

To locate the damages, the delay-and-sum imaging algorithm is applied with the cooperation of the valid data extraction strategy. A nonlinear normalization is performed to stand out the high pixel value in the damage image.[19] Fig. 6 gives the illustration of the damage images of the monitoring area and the star symbol represents the actual location of damage. As is shown in Fig. 6(a), the damage image is obtained with the original residual signals directly. The localization accuracy is dramatically deteriorated by the reflection of Lamb waves. Fig. 6(b) illustrates the damage image which is obtained with valid data extraction. It can be seen the localization accuracy is significantly improved by the proposed strategy.

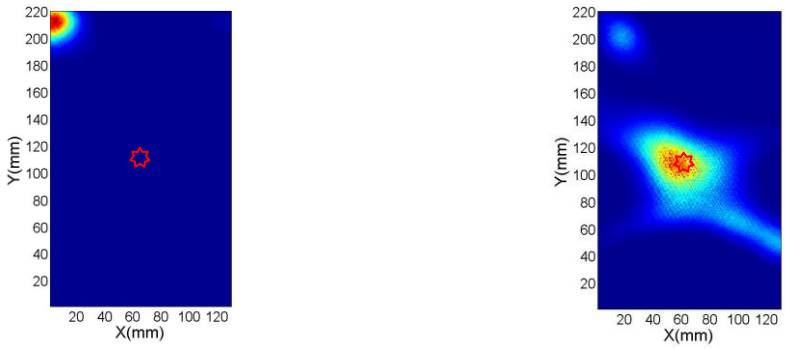

(a) (b)

Figure 6. (a) The damage image using residual signals directly; (b) the damage image using residual signals processed by valid data extraction

4.2 Evaluation of localization accuracy

According to equation (10), some typical deviations of the velocity are set to the system and the corresponding localization error distributions are calculated and shown in Fig. 7. From the results, a number of features of the imaging algorithm can be highlighted:

1. The localization error of a point in the monitoring area is closely related to its position. If damage locates near the center of the monitoring area, the localization error is less sensitive to preset velocity deviation. In other words, central damages can be located more accurately.

2. When the deviation is getting larger, the absolute value of the localization error tends to become larger. However, the localization error distribution of the monitoring area hardly changes.
3. There is some difference between the localization error distributions in the positive and negative deviation situations. Specially, when damage locates near the edges of the monitoring area, huge sensitivity difference between the two situations can be observed.
4. The maximum value of the localization error is about 25 mm when the preset velocity variation is up to 8%. In addition, when the deviation of velocity is within the range of ±5%, which is matched by the measured velocity deviation in this study, the maximum value of localization error is about 15 mm. Since the calculated damage covers a certain area in the image and the damage itself has a fixed size, the localization error is acceptable in engineering applications. As a result, it can be concluded the damage image method shows the great ability of robustness to the preset velocity variation.

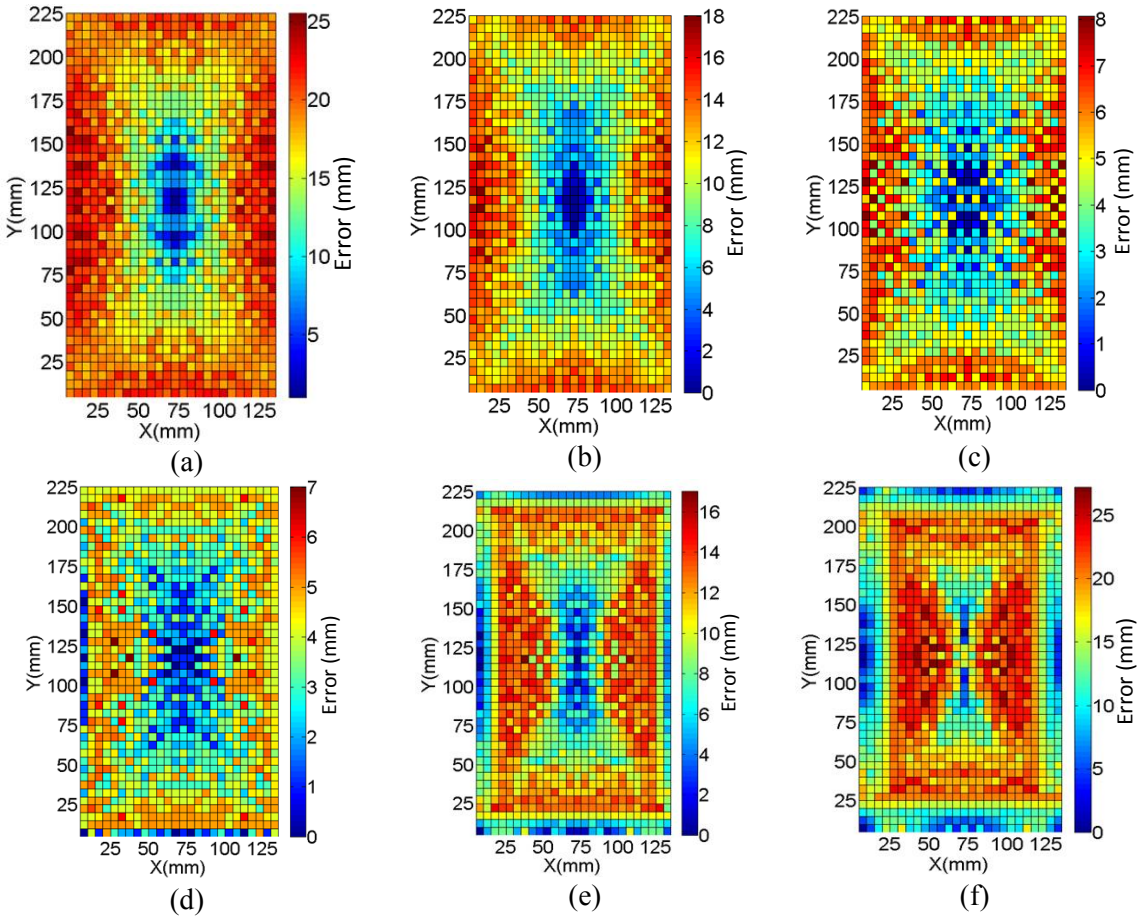

Figure 7. Localization accuracy distribution when a (a) -8%; (b) -5%; (c) -2%; (d) +2%; (e) +5%; (f) +8% deviation is added to the actual velocity

The localization error caused by preset velocity variation is researched in the experiment. Artificial damage is placed on the district where localization error is relatively more sensitive to the velocity variation. Fig.8 gives the illustrations of the damage images of the monitoring area obtained by setting different velocities to the monitoring system. In this case, the measured average velocity (1139 m/s) is considered as the actual group velocity of Lamb wave in the structure for all directions. The deviations are based on this average value. As is mentioned before, the deviation of velocity in the three directions is within the range of ±5%. When there are ±2.5%, 0%, ±5% deviation in the preset group velocity, damage

imaging process is carried out in these situations to analyze the corresponding localization errors. As is shown in Fig. 8(c), the localization accuracy is fairly excellent when choosing the average value of the measured velocities in the three directions. When the deviation is getting larger, the localization accuracy becomes poorer as is predicted in the former discussion. However, within the velocity deviation range from -5% to +5%, the localization error is less than 20 mm. In fact, taking the size of damage into consideration, the calculated damage zones in all the situations overlap with the actual damage. As a result, the system with the damage imaging algorithm has the satisfactory robustness to the preset velocity deviation. In addition, it is proved this velocity-choice approach for the system is both reasonable and effective.

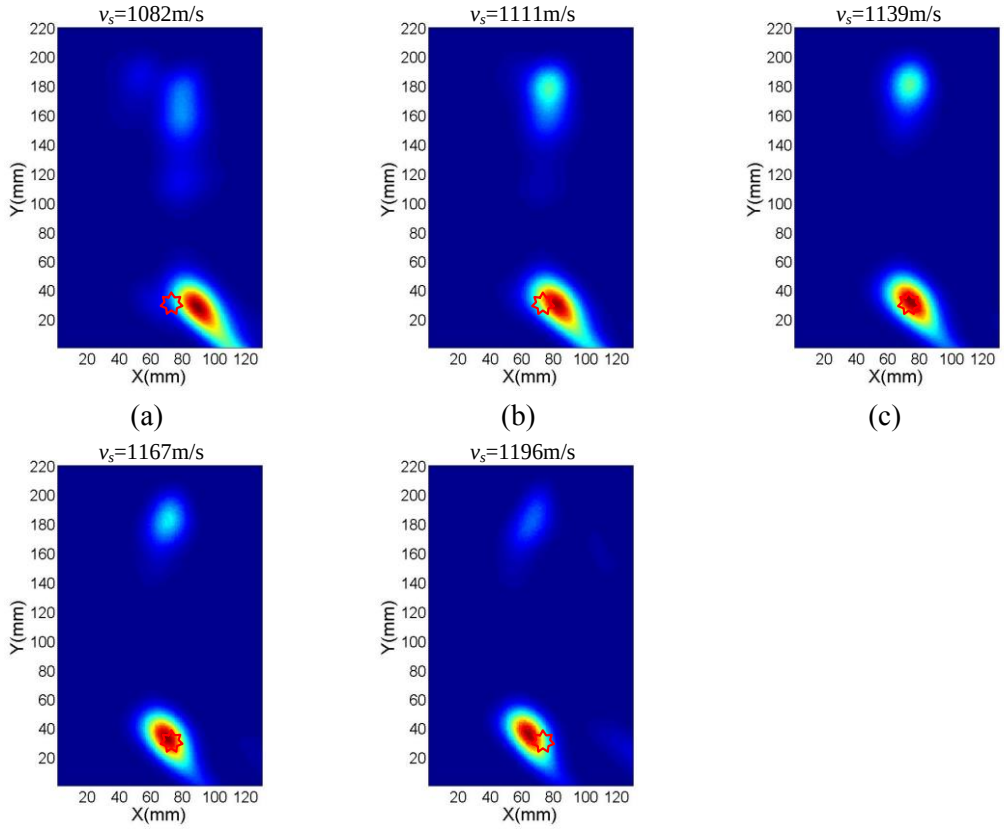

Figure 8. Damage images of the monitoring area obtained by different preset velocities: (a) -5%; (b) -2.5%; (c) 0%; (d) +2.5%; (e) +5%; deviation from the actual velocity

5. CONCLUSIONS

A damage monitoring method for a composite stiffened panel is proposed to locate the damage in the monitoring area. It provides a promising idea for SHM researches that the delay-and-sum algorithm along with the valid data extraction strategy can locate the damage accurately for complex structures with complex boundary conditions. It is an adaptive method as the monitoring radius of the actuator-sensor path is designed according to the geometric properties of the monitoring area. In addition, the influence of the preset velocity on the localization accuracy is evaluated to validate the robustness of the monitoring method. It is demonstrated that the preset velocity-choice method is effective for damage monitoring of

the quasi-isotropic structure. The results are of great significance for further engineering application of the proposed method.

ACKNOWLEDGMENTS

This work was supported by the National High Technology Research and Development Program of China (863 Program) (grant number 2013AA041105), the Foundation of Graduate Innovation Center in NUAA (grant number kfjj20130202) and the Fundamental Research Funds for the Central Universities.

REFERENCES

1. Soutis, C., "Fibre reinforced composites in aircraft construction," *Progress in Aerospace Sciences*, Vol. 41, No. 2, 2005, pp: 143-151.
2. Shanyi, D. U., "Advanced composite materials and aerospace engineering," *Acta Materiae Compositae Sinica*, Vol. 24, No. 1, 2007, pp: 1-12.
3. Cawley, P. and David A., "The use of Lamb waves for the long range inspection of large structures," *Ultrasonics*, Vol. 34, No. 2, 1996, pp: 287-290.
4. Staszewski, W. J., Boller, C. and Tomlinson, G., *Health monitoring of aerospace structures: smart sensor technologies and signal processing*, Chichester: John Wiley & Sons, 2004.
5. Boller, C., "Next generation structural health monitoring and its integration into aircraft design," *International Journal of Systems Science*, Vol. 31, No. 11, 2000, pp: 1333-1349.
6. Su, Z. and Ye, L., *Identification of damage using Lamb waves: from fundamentals to applications.* Berlin: Springer, 2009.
7. Masserey, B. and Fromme, P., "Fatigue crack growth monitoring using high-frequency guided waves," *Structural Health Monitoring*, Vol. 12, No. 5-6, 2013, pp: 484-493.
8. Miao, X.T., *Research of feature extraction technology and damage identification method for guided-wave-based structural health monitoring*. PhD Thesis, Shanghai Jiaotong University, Shanghai, 2011.
9. Clarke, T., Simonetti, F. and Cawley, P., "Guided wave health monitoring of complex structures by sparse array systems: influence of temperature changes on performance," *Journal of Sound and Vibration*, Vol. 329, No. 12, 2010, pp: 2306-2322.
10. Lu, Y. and Michaels, M., "A methodology for structural health monitoring with diffuse ultrasonic waves in the presence of temperature variations," *Ultrasonics*, Vol. 43, No. 9, 2005, pp: 717-731.
11. Dalton, R., Cawley, P. and Lowe, M., "The potential of guided waves for monitoring large areas of metallic aircraft fuselage structure," *Journal of Nondestructive Evaluation*, Vol. 20, No. 1, 2001, pp: 29-46.
12. Schubert, K. and Herrmann, A., "On the influence of moisture absorption on Lamb wave propagation and measurements in viscoelastic CFRP using surface applied piezoelectric sensors," *Composite Structures*, Vol. 94, No. 12, 2012, pp: 3635-3643.
13. Paget, C., *Active health monitoring of aerospace composite structures by embedded piezoceramic transducers*. PhD Thesis, Royal Institute of Technology, Stockholm, 2001.
14. Wang, C. H., Rose, J. T. and Chang, F. K., "A synthetic time-reversal imaging method for structural health monitoring," *Smart materials and structures*, Vol. 13, No. 2, 2004, pp: 415-423.
15. Michaels, J. E., "Detection, localization and characterization of damage in plates with an in situ array of spatially distributed ultrasonic sensors," *Smart Materials and Structures*, Vol. 17, No. 3, 2008, pp: 1-15.

16. Lu, Y., Ye, L., Wang, D., et al., "Conjunctive and compromised data fusion schemes for identification of multiple notches in an aluminium plate using lamb wave signals," *IEEE Transactions on Ultrasonics, Ferroelectrics, and Frequency Control*, Vol. 57, No. 9, 2010, pp: 2005-2016.
17. Ng, C. T. and Veidt, M., "A Lamb-wave-based technique for damage detection in composite laminates," *Smart materials and structures*, Vol. 18, No. 7, 2009, pp: 1-12.
18. Wang, Q., Yuan, S. F., Qiu, L., et al., "A time-reversal imaging method based on piezoelectric array technique for structure health monitoring," *Measurement & Control Technology*, Vol. 27, No. 2, 2008, pp: 8-10.
19. Qiu, L., Liu, M. L. , Qing, X. L., et al., "A quantitative multidamage monitoring method for large-scale complex composite," *Structural Health Monitoring*, Vol. 12, No. 3, 2013, pp: 183-196.
20. Lin, J. and Qu, L. S., "Feature extraction based on morlet wavelet and its application for mechanical fault diagnosis," *Journal of sound and vibration*, Vol. 234, No. 1, 2000, pp: 135-148.